Optical self cooling of a deformable Fabry-Perot cavity in the classical limit

Constanze Metzger,[*] Ivan Favero,[†] Alexander Ortlieb, and Khaled Karrai[‡]
Center for NanoScience and Fakultät für Physik, Ludwig-Maximilians-Universität, Geschwister-Scholl-Platz 1, 80539 München, Germany
(Received 27 July 2007; revised manuscript received 17 January 2008; published 9 July 2008)

We investigated the optomechanical properties of a Fabry-Perot cavity with a mirror mounted on a spring. Such a structure allows the cavity length to change elastically under the effect of light-induced forces. This optomechanical coupling is exploited to control the amplitude of the mechanical fluctuation of the mirror, a situation referred to as optical self cooling or passive optical cooling. We present a model developed in the classical limit and discuss data obtained in the particular case in which photothermal forces are dominant.

DOI: 10.1103/PhysRevB.78.035309 PACS number(s): 05.40.Jc, 07.10.Cm, 42.65.Sf, 07.57.Kp

I. INTRODUCTION

Photoinduced forces acting on a spring-mounted mirror are known to affect its dynamics.[1–18] We built a miniature Fabry-Perot (FP) cavity with a movable mirror held on a spring while the other mirror was massive enough to be static. The flexible mirror is compliant, so that it moves under the influence of light-induced forces originating from radiation pressure or photothermal forces that build up in the cavity. Such forces depend on the light intensity stored in the cavity, and their exact magnitude is determined by the cavity's mirror separation in proportion to the optical FP resonances. Consequently, any displacement of the mirror, resulting, for example, from thermal fluctuations, leads to a change in the light-induced force, inducing in return a change in the mirror position. This optomechanical coupling is referred to as intrinsic light-induced back action.[1]

An optical back action mechanism shifting the resonance frequency and adding damping on a mechanical resonator was first reported by Braginsky and Manukin[1] three decades ago. Optical back action remained a field of interest, especially in the research area of gravitational wave detection.[2,3] Gravitational wave detectors, mostly Michelson interferometers (for example, LIGO, a Michelson interferometer with arm lengths of 4 km that is illuminated with a 6 W Nd-doped yttrium aluminum garnet (YAG) laser beam[19]), are prone to get unstable because of optical back action. Instabilities were reported as well in smaller scale systems. A centimeter sized mirror hung on strings and serving as one mirror of a FP cavity showed mechanical instability under few watts of illumination.[5] More recently, back action was reported in microscale systems[9,18] When the photon back action force is delayed in time with respect to changes in mirror position, additional dissipation in the mirror's motion occurs without any additional mechanical fluctuations. The enhanced dissipation leads to reduced vibrational fluctuation and temperature of the mirror,[4,7–10] a situation referred to as passive optical cooling or self cooling.[4] Quantum mechanical behavior of a miniature mirror is expected[6] when the optical cooling becomes efficient enough to cool the mirror near its vibrational ground state. Experiments using a combination of photothermal forces and radiation pressure to cool a micromirror passively reach a temperature range of about 10 K, as shown in Refs. 4, 7, and 8. Optical cooling dominated by radiation pressure has been demonstrated not only in FP cavities[7,8] but in silica microtoroids[9] with a diameter in the range of 100 μm as well. Unfortunately, optical cooling mechanisms start to become inefficient as soon as the mirror reaches a size smaller than the diffraction limit of light in the cavity. Nevertheless, cooling of a micromirror with a diameter in the range of the laser wavelength was recently successfully demonstrated.[10]

In analogy to optical cooling, capacitative cooling of a nanomechanical resonator through charge coupling with a superconducting single-electron transistor was shown.[20] For a review, see Ref. 21.

In a pioneering work and in contrast to passive cooling mechanisms, Cohadon *et al.*[11] demonstrated the possibility of optical active cooling using an external electronic feedback loop in their system. In an earlier set of data by Mertz *et al.*,[12] optically induced damping by active feedback was observed. In cold damping schemes, a laser beam is directed toward the flexible mirror and can displace it by exerting radiation pressure[11] or a photothermal force.[12] The velocity of the mirror is detected and the laser intensity is adjusted by an electronic feedback loop in an appropriate way.[13,14] In principle, because this technique modulates the light intensity in proportion to a signal derived from the mirror amplitude noise, it adds technical fluctuations in the system. Using active optical cooling, up to now effective temperatures in the millikelvin range could be reached[15,22,23] with a vibrating mirror starting from room temperature. Recently, active cooling of a cantilever from 2.2 K down to about 3 mK was observed[17] using not optical but mechanical feedback forces.

In this paper, we present a model describing passive optical cavity cooling in a classical approximation and report on the passive cavity cooling of a micromirror by photothermal back action forces under various experimental conditions. In Sec. II, we present solutions to the equation of motion of a mirror with a delayed light-induced force acting on it. A derivation of the vibrational temperature of a mirror cooled by photoinduced forces is given in Sec. III. Section IV describes the mirror's equation of motion under a weakly modulated light-induced force. Different micro-FP experiments giving rise to optical cooling are presented in Secs. V and VI. Finally, in Sec. VII we compare the cooling power for different light-induced forces. We discuss the possibility that cooling by photothermal effects allows reaching lower temperatures compared to cooling by radiation pressure.

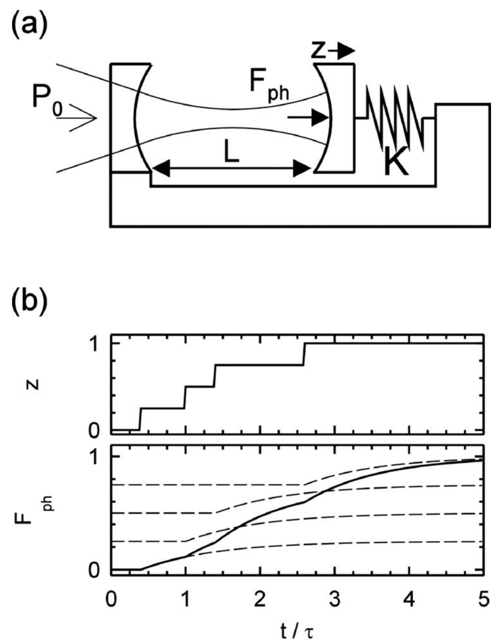

FIG. 1. (a) Schematic model of a deformable Fabry-Perot cavity. (b) After discreet step-shaped changes in mirror distance z, the light-induced force F grows after a characteristic delay time τ.

II. EQUATION OF MOTION UNDER CONSTANT ILLUMINATION

In this section, we solve the equation of motion of a vibrating harmonic oscillator forming a mirror of a FP cavity in the limit of small vibrational amplitudes. In our setup, a laser beam is coupled into the cavity through a fixed semi-transparent input mirror. Depending on the mirror distance, a resonance builds up in the cavity. The photons stored in the deformable FP cavity exert a force F_{ph} on the compliant mirror originating on the light field present in the cavity. The force is therefore directly dependent on the laser power and can be caused by any photon-induced force such as radiation pressure, photothermal deformation of the mirror, or radiometric pressure. For sake of generality, F_{ph} in our analysis is assumed to be any possible photon-induced force that is proportional to the local light intensity at the location of the mirror. Generally, such forces do not respond instantaneously to a change in mirror position; instead they show a delayed response with a time constant τ. For example, the finite photon storage time of a cavity accounts for the delay of radiation pressure forces with respect to a change in cavity length, while photothermal action on the mirror is retarded by the time it takes to conduct heat conduction along the mirror. These retardation mechanisms mimic the retardation vital for cooling of single atoms[24,25] that is determined by the radiative lifetime of single atoms.

A model system with a cantilever mirror that is able to move under the influence of a delayed photon force is shown in Fig. 1(a). We consider the equation of motion for the center-of-mass position z of a oscillator with an effective mass m, mechanical damping Γ, and spring constant K. The mirror thermal fluctuations are assumed to be driven by an thermal Langevin force F_{th},

$$m\ddot{z}(t) + m\Gamma\dot{z}(t) + Kz(t) = F_{\mathrm{th}}(t) + F_{\mathrm{ph}}(z(t)). \tag{1}$$

In the following, we model the total light-induced force on the cantilever. To illustrate, we consider that the cantilever position fluctuates in random increments under the effect of thermal excitations. The photon force responds retarded in time. After a step of $z_n - z_{n-1}$ at time t_n, the light-induced force F_{ph} follows with a delay of time τ as depicted in Fig. 1(b). If we were to stop the random motion of the mirror at step n, the light-induced force would reach asymptotically the static value $F(z_n)$. To model the behavior of $F_{\mathrm{ph}}(z(t))$ after N steps in mirror position, we sum up all force increments such that

$$F_{\mathrm{ph}}(z_N(t)) = F(z_0) + \sum_{n=1}^{N} h(t-t_n)[F(z_n) - F(z_{n-1})], \tag{2}$$

where the function $h(t)$ describes the time delay. This discrete sum can be reformulated as a continuous integral in time,

$$F_{\mathrm{ph}}(z(t)) = F(z_0) + \int_0^t dt' \frac{dF(z(t'))}{dt'} h(t-t'). \tag{3}$$

The equation of motion we need to solve then reads as

$$m\ddot{z}(t) + m\Gamma\dot{z}(t) + Kz(t) = F_{\mathrm{th}}(t) + F(z_0) + \int_0^t dt' \frac{dF(z(t'))}{dt'} h(t-t'). \tag{4}$$

This equation[4] leads to complex dynamics with multistability points treated in a recent work by Marquardt *et al.*[16] Here we focus on optical cooling, so for all practical purposes we assume the mirror amplitudes to be small compared to the change in cavity length needed for the optical resonance condition to change substantially. In terms of the FP cavity finesse $F=(\pi/2)g$, with $g=2\sqrt{R}/(1-R)$, this constraint translates into $z \ll \lambda/(2\pi g)$, where R is the reflectivity of the cavity mirrors.

Equation (4) is solved by Laplace transform, which is defined for a function $f(t)$ as

$$f_\omega = \int_0^\infty dt f(t) e^{-i\omega t}. \tag{5}$$

The constant force term $F(z_0)$ in Eq. (4) has no time dependence and simply leads to a static shift of the oscillator's average position. By selecting the new average position for z, it can be dropped from Eq. (4). The Laplace transform of Eq. (4) yields

$$-m\omega^2 z_\omega + i\omega m\Gamma z_\omega + Kz_\omega = \int_0^\infty dt e^{-i\omega t}\left[F_{\mathrm{th}}(t) + \int_0^t dt' \frac{dF(z(t'))}{dt'} h(t-t')\right]. \tag{6}$$

As $F(z(t'))$ depends on time indirectly through $z(t')$, its derivative in Eq. (6) is rewritten as

$$dF(z(t'))/dt' = \frac{\partial F(z(t'))}{\partial z}\frac{\partial z(t')}{\partial t'}. \tag{7}$$

In accordance with the small amplitude approximation, $F(z(t'))$ is developed in a Taylor expansion around $z(t_0)$: $F(z(t')) \approx F(z(t_0)) + [z(t') - z(t_0)]\nabla F$, where we use the abbreviation $\partial F(z(t'))/\partial z|_{z=z(t_0)} = \nabla F$. In the small amplitude fluctuation approximation, the partial derivative $\partial F(z(t'))/\partial z$ is now approximated with ∇F. We can reformulate Eq. (6) as follows:

$$-m\omega^2 z_\omega + i\omega m\Gamma z_\omega + Kz_\omega = F_{\mathrm{th},\omega} + \int_0^\infty dte^{-i\omega t}\left[\int_0^t dt'\,\nabla F\frac{\partial z(t')}{\partial t'}h(t-t')\right]. \tag{8}$$

With the property of Laplace transform for convolutions,

$$\int_0^\infty dte^{-i\omega t}\left[\int_0^t dt' f_1(t')f_2(t-t')\right] = f_{1,\omega}f_{2,\omega}, \tag{9}$$

Eq. (8) is reformulated as

$$-m\omega^2 z_\omega + i\omega m\Gamma z_\omega + Kz_\omega = F_{\mathrm{th},\omega} + \nabla F i\omega z_\omega h_\omega. \tag{10}$$

We assume that the shape of the delay function is of exponential type,

$$h(t) = 1 - e^{-t/\tau}. \tag{11}$$

This is reasonable because $h(t)$ describes the time scale the cavity system needs to approach a new equilibrium state after a disturbance. For instance, radiation pressure reacts with an exponential behavior. The other process considered in this work, the heat flow in an absorbing mirror after a change in cavity length, has an exponential response as well. The Laplace transform of the response function $h(t)$ is given by

$$h_\omega = \frac{1}{i\omega(1+i\omega\tau)}. \tag{12}$$

The terms in the right-hand side of Eq. (10) can be regrouped in powers of ω and Eq. (10) is rewritten as

$$-m\omega^2 z_\omega + i\omega m\Gamma_{\mathrm{eff}} z_\omega + K_{\mathrm{eff}} z_\omega = F_{\mathrm{th},\omega}, \tag{13}$$

with an effective damping

$$\Gamma_{\mathrm{eff}} = \Gamma\left(1 + Q_M\frac{\omega_0\tau}{1+\omega^2\tau^2}\frac{\nabla F}{K}\right), \tag{14}$$

and an effective spring constant

$$K_{\mathrm{eff}} = K\left(1 - \frac{1}{1+\omega^2\tau^2}\frac{\nabla F}{K}\right). \tag{15}$$

In Eq. (14), we used the vibrational harmonic resonance frequency of the center of mass of the mirror $\omega_0^2 = K/m$ and we defined the mechanical quality factor such that

$$Q_M = \frac{\omega_0}{\Gamma}. \tag{16}$$

Both the effective damping and rigidity are unusual in that they now include a frequency dependent term. The frequency dependency is that of a low-pass filter that ensures that at very high frequencies the retarded back action has no effect on the properties of the harmonic oscillator. Above cutoff the oscillating mirror behaves as if it was placed in the dark. In the limit of low frequencies (static limit), the effective damping and spring rigidities are constant; as a result, the solution of the equation of motion is that of an harmonic oscillator with optically modified frequencies and quality factor. For applications involving laser cooling of the lowest mechanical vibrational mode, the frequency range of interest is $\omega \approx \omega_0$, the cantilever's resonance frequency. We define the effective resonance frequency as

$$\omega_{\mathrm{eff}}^2 = \omega_0^2\left(1 - \frac{1}{1+\omega^2\tau^2}\frac{\nabla F}{K}\right), \tag{17}$$

where $\omega_{\mathrm{eff}}^2 = K_{\mathrm{eff}}/m$. The solution for the amplitude in the frequency domain of the harmonic oscillator is

$$z_\omega = \frac{F_{\mathrm{th},\omega}}{m}\frac{1}{\omega_{\mathrm{eff}}^2 - \omega^2 + i\omega\Gamma_{\mathrm{eff}}}. \tag{18}$$

It is important to note that we did not take into account that $h(t)$ is a function of the cavity detuning, in contrast to the model in Ref. 8. In our simplified approach, with low finesse cavities the effect of detuning on $h(t)$ is not measurable but becomes significant at high finesses.[8,9] The delay time of photothermal forces is entirely determined by heat conduction in the mirror and is not dependent on cavity detuning at all.

III. EFFECTIVE TEMPERATURE

In thermodynamical equilibrium without illumination and any light-induced effects, the average power in the mechanical ground mode of the mirror center-of-mass motion is described by the equipartition theorem,

$$\frac{1}{2}K\int_0^\infty dt|z_{\mathrm{dark}}(t)|^2 = \frac{1}{2}k_BT. \tag{19}$$

Here k_B is Boltzmann's constant and T is the bath temperature. An important property of Laplace transforms is that the integrated Laplace coefficients $\int d\omega|z_\omega|^2$ equal the time average,

$$\int_0^\infty d\omega|z_{\mathrm{dark},\omega}|^2 = \int_0^\infty dt|z_{\mathrm{dark}}|^2. \tag{20}$$

This expression provides the prescription for performing vibrational thermometry, namely, a method to extract temperature from the measurement of the spectral distribution of the Brownian motion of the mirror. First, the rigidity K must be determined independently, such as, for instance, by measuring the resonance frequency knowing the oscillator effective mass. Then, the spectrum of the fluctuation amplitude z_ω is measured on a sufficiently extended frequency range around the vibrational resonance frequency and averaged over a large enough number of measurements. Finally, the integration of $|z_\omega|$ multiplied by the rigidity gives the thermal energy experienced by the harmonic oscillator and hence the temperature. We will use this prescription later on to determine the temperature of the mirror coupled to the optical cavity. The expression for the frequency averaged square modulus of the amplitude can be now computed using the solution z_ω of Eq. (18) but still as a function of the still nonexplicitly expressed thermal fluctuation force component $F_{\mathrm{th},\omega}$. In the absence of light in the cavity, the equipartition theorem gives us already the opportunity to derive the expression of $F_{\mathrm{th},\omega}$ that we can then finally use to obtain the dynamics of the mirror with light in the cavity. As we will see shortly, the result will be that the mirror fluctuates in a way nearly identical to the Brownian motion of the original harmonic oscillator in the dark but with a modified temperature induced by the presence of light in the cavity. In the dark, setting all light-induced effects to zero in Eq. (1) for z_ω, we have

$$z_{\mathrm{dark},\omega} = \frac{F_{\mathrm{th},\omega}}{m}\frac{1}{\omega_0^2 - \omega^2 + i\omega\Gamma}. \tag{21}$$

With the reasonable assumption that the spectral force density of thermal vibrations given by $F_{\mathrm{th},\omega}$ is equally distributed over all frequencies, one can calculate the strength of the thermal force. We assume that

$$|F_{\mathrm{th},\omega}|^2 = Sdf \tag{22}$$

in every frequency interval df with a constant spectral density S, which can be calculated in the next step by integrating Eq. (21) over all frequencies ω,

$$\int_0^\infty d\omega |z_{\mathrm{dark},\omega}|^2 = \int_0^\infty d\omega \frac{S}{2\pi m^2}\frac{1}{(\omega_0^2-\omega^2)^2+\omega^2\Gamma^2}. \tag{23}$$

The experimentally relevant assumption $\Gamma \ll \omega_0$ is made, so the integral simplifies to

$$\int_0^\infty d\omega |z_{\mathrm{dark},\omega}|^2 = \frac{S}{2\pi m^2 \Gamma^2 \omega_0^2}\int_0^\infty d\omega \frac{1}{4\left(\frac{\omega_0-\omega}{\Gamma}\right)^2+1}, \tag{24}$$

leading to the solution

$$\int_0^\infty d\omega |z_{\mathrm{dark},\omega}|^2 = \frac{S}{4K\Gamma m}. \tag{25}$$

With that result, the solution of the oscillator's spectrum [Eq. (25)] can be inserted in the equipartition theorem [Eq. (19)]. The driving fluctuation [Eq. (22)] is determined to be

$$|F_{\mathrm{th},\omega}|^2 = 4k_B T m \Gamma \frac{d\omega}{2\pi}. \tag{26}$$

Finally, the thermal noise spectrum of a harmonic oscillator in the dark is

$$|z_{\mathrm{dark},\omega}|^2 = \frac{4k_B T\Gamma}{m}\frac{1}{(\omega_0^2-\omega^2)^2+(\omega\Gamma)^2}\frac{d\omega}{2\pi}. \tag{27}$$

Now, we still need to find an expression for the thermal driving force $F_{\mathrm{th},\omega}$ in the solution of the equation of motion with light [Eq. (18)]. When the light is turned on, the spectral force density $F_{\mathrm{th},\omega}=Sdf$ is not influenced by the photon-induced force and Eq. (26) still holds because it is dependent only on the natural mechanical damping Γ and the undisturbed spring constant K. The spectral amplitude of a mirror under illumination is

$$|z_\omega|^2 = \frac{4k_B T\Gamma}{m}\frac{1}{(\omega_{\mathrm{eff}}^2-\omega^2)^2+(\omega\Gamma_{\mathrm{eff}})^2}\frac{d\omega}{2\pi}. \tag{28}$$

Integrating this over all frequencies and using the property of Laplace transforms in Eq. (20) gives

$$\int_0^\infty dt|z|^2 = \frac{\Gamma}{\Gamma_{\mathrm{eff}}}\frac{k_B T}{K_{\mathrm{eff}}}. \tag{29}$$

This averaged squared amplitude is related to a temperature T_{eff} via the equipartition theorem as follows:

$$\frac{1}{2}K_{\mathrm{eff}}\int_0^\infty dt|z|^2 = \frac{1}{2}k_B T_{\mathrm{eff}}. \tag{30}$$

Solving this for the effective temperature and using Eq. (29) yields[11]

$$\frac{T_{\mathrm{eff}}}{T} = \frac{\Gamma}{\Gamma_{\mathrm{eff}}}. \tag{31}$$

No absorption of light in the mirror was taken into account up to now. Still, even dielectric mirrors possess a residual absorption leading to heating. If the temperature is increased considerably above the bath temperature, Eq. (31) needs to be corrected. The bath temperature T has to be substituted then with the temperature the mirror would reach in the absence of optical cooling $T+\Delta T$.

In a previous work,[4] we established that $T_{\mathrm{eff}}/T = (\Gamma/\Gamma_{\mathrm{eff}})(K/K_{\mathrm{eff}})$, which does not take into account that the effective temperature is determined by the squared noise amplitude $\int_0^\infty dt|z|^2$ multiplied by the independently measured effective spring constant K_{eff} instead of the unperturbed spring constant K. This correction creates a factor K_{eff}/K, yielding effective temperature equation (31).

With the help of Eq. (14), the result of Eq. (31) is reformulated as

$$\frac{T_{\mathrm{eff}}}{T} = \frac{1}{1+Q_M \frac{\omega_0\tau}{1+\omega^2\tau^2}\frac{\nabla F}{K}}, \tag{32}$$

revealing the physical parameters playing a role in cavity cooling.

The cooling stops when the static spring constant $K_{\mathrm{eff}}(\omega=0)$ reaches zero and becomes negative. At this point, mirror bistability sets in[18] and no stable measurement is possible any more. Consequently, a theoretical limit of cooling is obtained for $K_{\mathrm{eff}}=K(1-\nabla F/K)=0$ in Eq. (32) and considering the optimal case of $\omega_0\tau=1$,

$$\frac{T_{\mathrm{eff,limit}}}{T} = \frac{1}{1+Q_M/2}. \tag{33}$$

This expression shows that the mechanical quality factor Q_M, which relates to the ability of the mechanical mode to dissipate its energy, plays a central role for the optical cooling mechanism.

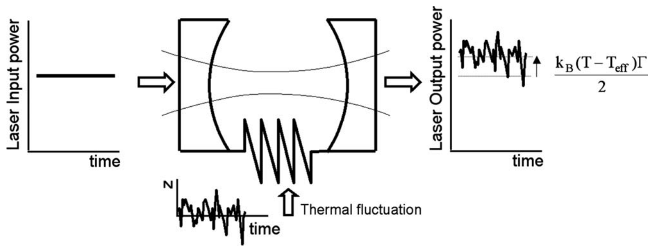

FIG. 2. A FP cavity with a mirror attached on a spring is illuminated with a laser beam. The input laser intensity is assumed to be noiseless. The transmitted light shows amplitude fluctuations, which are impressed on the original amplitude by the thermal fluctuation of the mirror. More importantly, the transmitted laser light has an averaged intensity enhanced by the fluctuations added by the mechanical resonator. The mirror vibrational motion has been cooled and the excess energy turns into photons.

According to Eq. (31) the lowest effective temperature is entirely driven by the damping modified through the cavity effect. In turn, this modification in damping exists only if a time delay exists between the motion of the mirror and the resulting change in the light-induced force it experiences; see Eq. (14). Thus the essence of optical cooling finds its root on the retarded back action on the mirror displacement.

Up to now, we did not offer an explanation as to where the thermal energy extracted from the vibrating cantilever goes. It turns into the fluctuation of the electromagnetic field escaping the cavity as shown in Fig. 2. The system formed by the mechanical oscillator and the electromagnetic field remains at constant energy. We offer a possible picture on how this happens. The fluctuating cavity length modulates the photon frequency at all frequencies but with amplitude maxima at the vibrational resonance frequency. Such amplitude modulation of the light field produces side bands above and below the photon frequency with peaks shifted on both sides by the vibrational resonance of the mirror (in Raman spectroscopy they would be Stokes and anti-Stokes resonances).[26] When the laser is red detuned from the cavity transmission maximum, the band with shorter wavelength is closer to the transmission peak. Seen from the outside world, a detector would measure a fluctuating irradiance imbalance between the side bands as more blueshifted light is reaching the detector than redshifted light. This excess of energy is given by the difference in transmitted light power between the blue and red sides of the band and this over the typical delay time constant for the light-induced force to correct against the mirror fluctuation. The excess energy has been taken away from the very source that produced the side bands to begin with, namely, the Brownian fluctuation of the mirror. In this picture, the cooling is optimal when the frequency width of the cavity, that is, the inverse storage time $1/\tau$, is comparable to the side-band frequency separation from the laser light frequency, in other words when $\omega_0\tau \approx 1$. This picture seems to be consistent with the model and in particular, it is easy to see that with a zero time delay the net excess energy is also zero and no cooling is possible. An alternative picture possibly more appropriate to photothermal cooling is the following: The laser light is tuned to be redshifted from a transmission peak of the cavity. When the cavity length fluctuates and say becomes shorter over a certain time period, the transmission peak gets closer to the laser line and more light can be stored in the cavity during that time. The result of the excess light is to exert more pressure on the mirror as to oppose the cavity from becoming even shorter. In the opposite case, when the cavity gets longer upon a thermal fluctuation, the averaged steady-state light pressure that displaced the mirror from its position in the dark reduces and the mirror tends to move back under its own restoring elastic force as to oppose this very fluctuation. The retarded back action makes this force oppose the mirror velocity dz/dt and not only its instantaneous position z. It is therefore a dissipative force and during the typical response time, energy is irreversibly lost to the light field outside the cavity. In this picture the cavity serves as a reservoir of energy stored in form of light, and the rate of energy leakage from this reservoir is fully controlled by the mirror kinetics. Energy conservation dictates that mechanical energy can be transformed into energy that escapes the reservoir in form of light.

IV. EQUATION OF MOTION UNDER MODULATED ILLUMINATION

The solution of the equation of motion of a mirror under the influence of light-induced forces in Sec. II is generalized for a weakly modulated light-induced force. This modification proves to be useful because a measurement with modulated laser light opens up the possibility to measure the magnitude of the light-induced force as well as its delay time. The technique makes is possible to determine if either radiation pressure, photothermal pressure, or even a summation of both effects is responsible for the observed cooling effects. We took advantage of this method in a modulated laser measurement that is discussed in Sec. V.

If the laser intensity is weakly modulated, the light-induced force is described by

$$F(z(t),t) = (1+\varepsilon(t))F_{\rm ph}(z(t)), \tag{34}$$

with a small modulation strength $\varepsilon(t) \ll 1$. The light-induced force has now an explicit dependence on t and differs from Eq. (3) as follows:

$$F(z(t),t) = F_{\rm ph}(z_0) + \int_0^t \left(\frac{\partial F_{\rm ph}}{\partial t'} + \frac{\partial F_{\rm ph}}{\partial z}\frac{\partial z}{\partial t'}\right) h(t-t')dt'. \tag{35}$$

The solution for the amplitude is

$$z_\omega = \left(\frac{F_{{\rm th},\omega}}{m} + \frac{F_{\rm ph}}{m}\frac{\varepsilon_\omega}{1+i\omega\tau}\right)\frac{1}{\omega_{\rm eff}^2 - \omega^2 + i\omega\Gamma_{\rm eff}}. \tag{36}$$

Compared to the solution without external excitation of the mirror [Eq. (18)], the amplitude has an additional term $(F_{\rm ph}/m)\varepsilon_\omega/(1+i\omega\tau)$. This term offers a way to extract both the delay time τ and the magnitude of the light-induced force $F_{\rm ph}$ from a measurement of the real part as well as the imaginary component of the response z_ω, so the measurement can be done with the aid of lock-in detection (see Sec. V) by

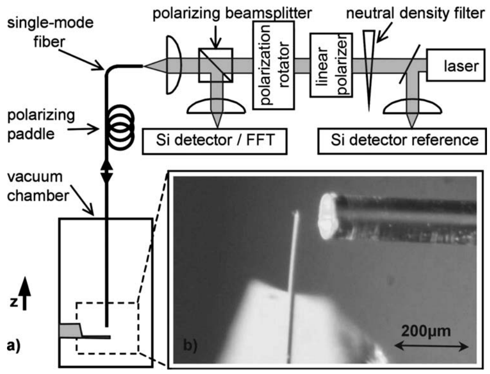

FIG. 3. (a) Schematic of the experimental setup. Inset (b) shows a photograph of a similar cavity as used in the experiment but with a lever to mirror separation greatly increased for the picture. During measurements, the cavity length was 34 μm.

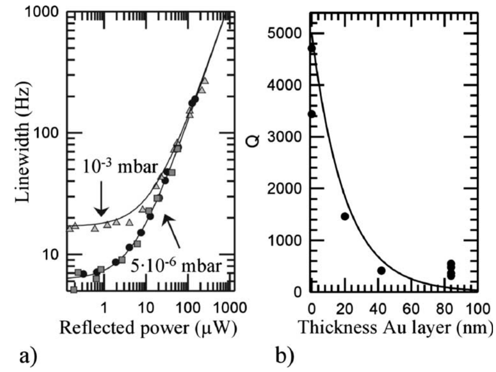

FIG. 4. (a) Dependence of the cantilever's resonance linewidth at full width at half maximum on pressure and laser power. The triangles show data taken with a HeNe laser at moderate pressure of about 10^{-3} mbar, while the circles show data taken at the minimum pressure of 5×10^{-6} mbar. The squares represent data taken also at the minimum pressure but using a red (670 nm) diode laser instead. Clearly, the linewidth of the cantilever is much smaller at 5×10^{-6} mbar. (b) Mechanical quality factors of different cantilevers with various thicknesses of evaporated gold. The gray line is a guide to the eye.

measuring the in- and out-of-phase component of the reflected light. Using Eq. (36) to model the data, the delay time of the force is extracted. Besides, if different light-induced forces such as radiation pressure and photothermal pressure are present in the setup, the ratio of different forces can be determined when their response times differ significantly.

In Secs. V and VI, we investigate in two different setups the optical cooling of the vibration modes of a gold coated atomic force microscope (AFM) silicon cantilever. In this system, the presence of the bilayer gives rise to a photothermal bending of the lever under illumination. The delay time of the light-induced force is the time of thermal response of the lever.

V. COOLING OF THE GROUND MODE

In this section, a setup displaying passive back action cooling is shown [see Fig. 3]. We used alternatively a red HeNe laser (Research Electro-Optics LHRP 1701, $\lambda=632.8$ nm, 17 mW) or a diode laser ($\lambda=670$ nm, 5 mW) beam coupled into a single mode optical fiber (numerical aperture, 0.13). The highly coherent HeNe laser was used for the vibrational resonance linewidth measurements shown in Fig. 4. For measurements involving laser amplitude modulation, we preferred using the diode laser because it could be easily modulated. A neutral density filter wheel allowed tuning the laser power continuously over almost 4 orders of magnitude. The reflected laser power was measured at the level of the Si detector and was varied from 35 nW to up to 150 μW. The fiber was introduced into a vacuum chamber operating down to a pressure in the 10^{-6} mbar range. Reaching this low enough pressure was important in order to reduce the damping of the cantilever, as shown in Fig. 4(a). The fiber end forming a cavity mirror in the vacuum chamber was thoroughly polished and coated with a gold film of 19 nm by thermal evaporation under high vacuum. A silicon cantilever (Nanosensors) with a width of 22 μm, a thickness of 0.47 μm, a length of 220 μm, and a spring constant of 0.008 N/m was mounted at a distance of 34 μm from the polished fiber end. Gold layers of 36 nm were deposited on each side of the lever. A simulation of the coated cantilever optical properties gave a reflectivity of 82% for a laser wavelength of 633 nm. The distance between fiber and cantilever was tuned by applying a dc voltage between them to create a capacitative force. About 15 V was required in order to detune the cavity through three resonances. The light reflected from the cavity was coupled back into the fiber. A fiber paddle polarizator was used to rotate the linear polarization of the reflected light in order to be directed by a polarizing beam splitter onto a Si photodetector and minimize back reflected light on the laser. We increased this way the collected efficiency by a factor of 4. A polarization rotator (B. Halle Nachf., $\lambda/2\pm1\%$ Fresnel rhombus, 400–700 nm) was used to align the laser polarization to the polarizing beam splitter.

In Fig. 5(a), the normalized reflectivity of the FP cavity is shown. The cavity finesse is about 4, which corresponds to $g=2.5$. Figure 5(b) shows the spectra of the cantilever fundamental harmonic at 7.3 kHz with effective temperatures of 300, 86, 64, and 32 K. All curves are taken at the same cavity detuning of $\Delta z=+\lambda/(2\pi g\sqrt{3})\approx\lambda/25$, for which one expects maximum gradient of the light-induced force, and therefore maximum cavity cooling.[18] At a very low reflected laser power of 3.1 μW, one measures the amplitude fluctuation spectral density near the vibrational resonance of the cantilever corresponding to a temperature of 300 K. A fit with Eq. (27) is obtained with the parameters $f=7265$ Hz, $K=2.5\times10^{-2}$ N/m, and $\Gamma=28$ Hz. At increased laser power of 3.6 mW, the effective damping is found to be $\Gamma_{\mathrm{eff}}=263$, which relates when using Eq. (31) to an effective temperature of 32 K for this set of data. So far the lowest temperature obtained with this setup[4] was 18 K. In order to achieve the highest possible cooling effect, different parameters have to be optimized as stated in Eq. (32).

First, the mechanical damping Γ of the cantilever needs to be minimized. The damping of a resonator includes several contributions such as clamping losses, defects in crystal

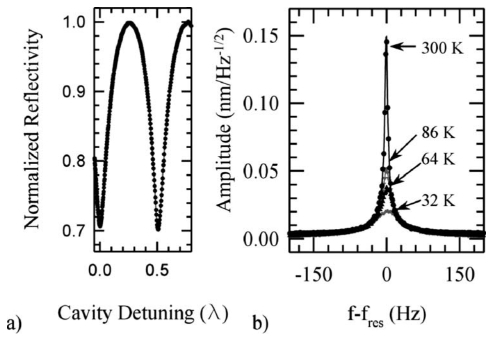

FIG. 5. (a) Normalized reflectivity of plan-plan cavity setup shown in Fig. 3. The cavity detuning is calibrated in units of the wavelength λ. The finesse is 4, with the parameter g=2.5. (b) Amplitude fluctuation spectral density near vibrational resonance of the cantilever with f_0=7.3 kHz with different laser powers taken at cavity detuning of +λ/25 from a cavity resonance. The largest amplitude corresponds to thermal fluctuation at 300 K with mechanical damping Γ=28 Hz, measured with reflected laser power of 3.1 μW. The other measurements correspond to reflected laser powers of 0.87, 1.3, and 3.6 mW with damping of Γ=98, 131, and 263 Hz. The effective temperatures of the spectra from top to bottom are 300, 86, 64, and 32 K.

structure, surface losses,[27] and damping due to scattering of air molecules. to name a few. The last one can be reduced by running the system in vacuum. A simple model of the gas damping can be found by assuming that the viscous damping by molecular scattering is $F_{\mathrm{visc}}=(Nm_N v)/t_{\mathrm{scat}}$, with N as the number of atoms scattering off the cantilever, $m_N=4.6\times10^{-26}$ kg as the mass of nitrogen atoms, $v=510$ m/s as the mean atomic velocity at 300 K, and t_{scat} as the mean scattering time. This approximation predicts that at a pressure of 10^{-3} mbar, molecular scattering should already account for 1% of the damping. In reality, we still see a sizable change in quality factor going from 10^{-3} mbar ($\Gamma=61.7$ Hz) to 5×10^{-6} mbar ($\Gamma=14.5$ Hz). The linewidth at full width at half maximum (FWHM) relates to the mechanical damping as FWHM$=\sqrt{3}\Gamma/(2\pi)$. We find a linewidth of 17 Hz corresponding to a quality factor of $Q_M=744$ for 10^{-3} mbar and a linewidth of 4 Hz ($Q_M=3161$) for 5×10^{-6} mbar, as shown in Fig. 4(a), at low reflected power. Evidently, the observed damping cannot be explained by molecular viscous damping alone. Molecular adsorption on the cantilever surface may be responsible for the additional damping; so at lower pressure, desorption could explain the improved quality factor. As seen in Eq. (14), the linewidth of the mechanical resonance is modified linearly with laser power as long as the photon-induced force is linear with intensity. In the cooling regime, it is broadened with increasing laser power starting from the natural linewidth at dark. In Fig. 4(a) the linear dependency of the linewidth on the reflected laser power is plotted in logarithmic scale for different chamber pressures, showing the smallest possible linewidth at low pressure and low laser power.

In order to maximize the cooling efficiency, a tradeoff between the reflectivity of the cantilever and its mechanical damping had to be made. Higher reflectivity should increase the cavity finesse and therefore lead to a stronger cooling effect, through both an increase in the light power circulating in the cavity close to resonance and an increase in its gradient upon position. Unfortunately, increasing the reflectivity by evaporating a thicker gold layer on the cantilever adds additional mechanical damping as well.[28] In our experiment we used different thicknesses of evaporated gold on many cantilevers of the same kind, the quality factor decreased by an order of magnitude, as shown in Fig. 4(b).

Second, to enhance the cooling efficiency, the parameter τ needs to be optimized. An inspection of Eq. (32) shows that optimum cooling is reached for $\omega\tau=1$. In case of thermal bending of the cantilever, the delay time of the light-induced force is given by the time it takes the thermal energy to diffuse along the cantilever. For a bilayer cantilever consisting of a thin gold layer with thickness u_{Au} and a silicon layer with thickness u_{Si}, this thermal diffusion time constant τ_{pth} can be approximated by[29,30]

$$\tau_{\mathrm{pth}} = l^2 \frac{\rho_{\mathrm{Si}} c_{\mathrm{Si}} u_{\mathrm{Si}} + \rho_{\mathrm{Au}} c_{\mathrm{Au}} u_{\mathrm{Au}}}{\Lambda_{\mathrm{Si}} u_{\mathrm{Si}} + \Lambda_{\mathrm{Au}} u_{\mathrm{Au}}}, \qquad (37)$$

with ρ as the density, c as the specific heat capacity, Λ as the thermal conductivity, and l as the length of the cantilever. Taking the parameters of the cantilever given above and $\rho_{\mathrm{Si}}=2.33$ g/cm^3, $\rho_{\mathrm{Au}}=19.3$ g/cm^3, $c_{\mathrm{Si}}=0.71$ J/(g K), $c_{\mathrm{Au}}=0.128$ J/(g K), $\Lambda_{\mathrm{Si}}=1.48$ W/(cm K), and $\Lambda_{\mathrm{Au}}=3.17$ W/(cm K), one finds $\tau_{\mathrm{pth}}=0.5$ ms. With the mechanical resonance frequency of the cantilever of $f_0=7.3$ kHz, a value of $\omega_0\tau=25$ is found. It is interesting to note that $\omega_0\tau$ is a function of material thickness alone. The resonance frequency of a multilayer cantilever is given by

$$\omega_0 = \frac{(1.875)^2}{l^2}\sqrt{\frac{1}{u_1\rho_1 + u_2\rho_2}\int_{-u/2}^{u/2} E(u-u_0)^2 du}, \qquad (38)$$

where u_0 denotes the cantilever's neutral stress axis. The Young modulus E is integrated over the thickness u of the different cantilever layers.[31] For a cantilever consisting of one layer, Eq. (38) simplifies to $\omega_0=u/l^2\sqrt{E/\rho}$ and the corresponding thermal constant is $\tau_{\mathrm{pth}}=l^2/h$, where $h=\Lambda/(\rho c)$ is the thermal diffusivity. Setting the condition $\omega\tau=1$ leads to an optimal thickness $u_{\mathrm{opt}}=h\sqrt{\rho/E}$. For silicon at room temperature, this optimal thickness is found to be 10 nm with $h=8.6\times10^{-5}$ m^2/s; the values were taken from Ref. 32. This value is far too small for fabrication of freestanding silicon structures. However, a diamond resonator with optimized thickness seams feasible. With $E_{\mathrm{diam}}=1.1\times10^{12}$ N/m^2, $\rho_{\mathrm{diam}}=3200$ kg/m^3, and $h_{\mathrm{diam}}=5.09\times10^{-4}$ m^2/s, one finds an optimal thickness of 27.5 nm. A resonator with that thickness and a length of 900 nm would feature a resonance frequency of 100 MHz. For a silicon cantilever, the temperature can be used to tune $\omega_0\tau$ since the specific heat c and the thermal conductivity Λ show strong temperature dependence and a temperature where $\omega_0\tau=1$ can be found. For example, the diffusivity of silicon[32] increases by a factor of 20 from 300 to 80 K, so placing the cantilever of our experiment at liquid-nitrogen temperature of 77 K should allow reaching the optimal condition $\omega_0\tau\approx1$, in contrast to $\omega_0\tau\approx25$ at room temperature.

For radiation-pressure-induced cooling, the delay time is given by the cavity storage time for a photon,[4] $\tau_R = L/[c(1-R)]$. With our parameters we find that the cavity storage time is in the range of 0.2 ps and therefore orders of magnitudes smaller than the thermal diffusion time constant. For this reason, in this experiment we expect optical cooling to be mostly dominated by photothermal effects and not by radiation pressure. In order to obtain the measured value $\tau_{\rm pth}$, we performed a response measurement of the cantilever's motion driven by a weakly modulated laser light-induced force. The laser intensity of a red diode laser with a wavelength of 670 nm was modulated weakly by modulating the laser current with a signal generator and we used the internal reference of a lock-in (SR 7265). About 5% of the overall intensity was modulated such that the modulation parameter ε in Eq. (34) was 0.05. The modulation frequency was swept in single steps in the frequency range from dc to 100 kHz. The reflected signal measured at the Si photodetector was demodulated using the lock-in. We were interested in measuring the imaginary part of the overall amplitude response shown in Eq. (36). The measurement of the real part of Eq. (36) for low laser amplitude is

$$\mathrm{Re}(z_\omega) = \frac{\varepsilon_\omega F_{\rm pth}}{m} \frac{\omega_0^2 - \omega^2(1+\Gamma\tau)}{[(\omega_0^2-\omega^2)^2 + \omega^2\Gamma^2](1+\omega^2\tau^2)}, \qquad (39)$$

without taking into account the contribution of $F_{\rm th}$, which is much smaller than $F_{\rm pth}$. The real part is always superimposed onto the amplitude of the modulated light intensity, εPR. This adds a complication in detecting the direct optomechanical effect. In contrast, the measurement of the imaginary part,

$$\mathrm{Im}(z_\omega) = \frac{\varepsilon_\omega F_{\rm pth}}{m} \frac{-\omega[(\omega_0^2 - \omega^2)\tau + \Gamma]}{[(\omega_0^2-\omega^2)^2 + \omega^2\Gamma^2](1+\omega^2\tau^2)}, \qquad (40)$$

is purely dependent on the optomechanical response.[10] In the experiment, we found two different competing forces. A photothermal force with a delay time in the range of heat diffusion time was coexistent with the quasi-instantaneous radiation pressure force.

The imaginary part shows a characteristic local maximum where the response function $\omega\tau/(1+\omega^2\tau^2)$ is maximal at the frequency $1/(2\pi\tau)$. In a modulated response measurement, one measures an overall phase shift occurring in the system. The phase shift is not only caused by the cantilever's response alone but also includes the phase shifts in the detection apparatus. To solve this technical problem, we devised a measuring procedure canceling spurious phase shift effects at all frequencies. For each measurement at a given modulation frequency, we first measured the spurious phase shifts by switching off all signals coming from the optomechanical response of the cantilever itself. This is obtained when the force gradient $\nabla F = 0$, so we tuned the cavity such that the reflectivity was maximum. The phase is then set to zero at the lock-in. In a next step, without changing any other parameter, we detuned the cavity to a regime of maximum ∇F. At this point, the imaginary component of the signal is solely originating from the cantilever optomechanical response. For each modulation frequency, we repeated the procedure explained above. The result is shown in Fig. 6. We were able to fit the data with Eq. (40) using a combination of two forces acting on the lever. The first is a thermal bending force with a time delay of $\tau_{\rm pth} = 560$ μs. The second is the quasi-instantaneous ($\tau \approx 0$) radiation pressure that does not contribute here to cooling. The ratio of the forces was found to be $F_{\rm pth}/F_{\rm rad} = -95$. On resonance, $\nabla F_{\rm pth}/(1+\omega_0^2\tau^2)$ is the contribution of the thermal force to the light-induced frequency shift. Its magnitude is found to be $95/625 = 0.15$ smaller than the contribution of $F_{\rm rad}$, so effects on frequency shift in this experiment were dominated by radiation pressure alone.[4] The modulated experiment shown in Fig. 6 demonstrated convincingly that the observed cooling effects were dominated not by radiation pressure but by a photothermal bending force that was 95 times stronger than radiation pressure and had an opposite sign. The value found experimentally for the delay time, $\tau = 560$ μs, is in agreement with the prediction of 0.5 ms made with the help of Eq. (37). This indicates that a small asymmetry in the thickness of the gold layers on the two faces of the cantilever creates a thermal force opposing the radiation pressure. The imaginary response shows a clear maximum at the cantilever resonance and an enhancement at the frequency $f = 1/(2\pi\tau) = 284$ Hz, corresponding to the thermal response of the system. We see that the cooling effect at the cantilever's ground mode of 7300 Hz is not optimal because $\omega_0\tau \approx 25$ is far from 1. As mentioned earlier, placing the lever at 77 K should optimize the cooling to $\omega_0\tau$ to about 1.

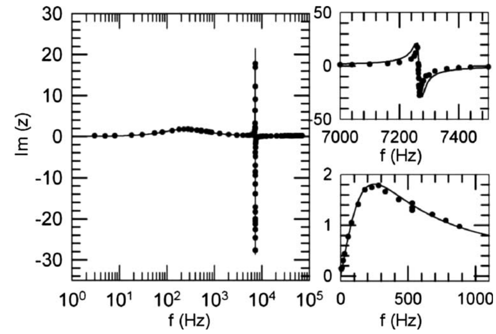

FIG. 6. Response measurement of driven cantilever amplitude. Frequency sweep is from 0 to 100 kHz. The upper inset shows a zoom of the region around the cantilever resonance frequency at 7.3 kHz. The inset at the bottom shows a zoom of the enhanced response at $f = 284$ Hz arising at the frequency where $\omega\tau = 1$. The response frequency corresponds to $\tau_{\rm pth} = 560$ μs.

VI. SIMULTANEOUS COOLING OF THE FUNDAMENTAL VIBRATIONAL MODE AND ITS FIRST HARMONIC

In an experiment using a cantilever with a gold coating on one side only, much stronger thermal forces were measured. Here, we used a slightly different cavity arrangement designed to increase the cavity finesse as well as to decrease the size of the laser beam on the microlever.

The light of a red monomode HeNe laser (Sios, $\lambda = 633$ nm, 1.3 mW) was coupled into a single mode fiber (NA=0.13). The fiber end was polished and coated with a

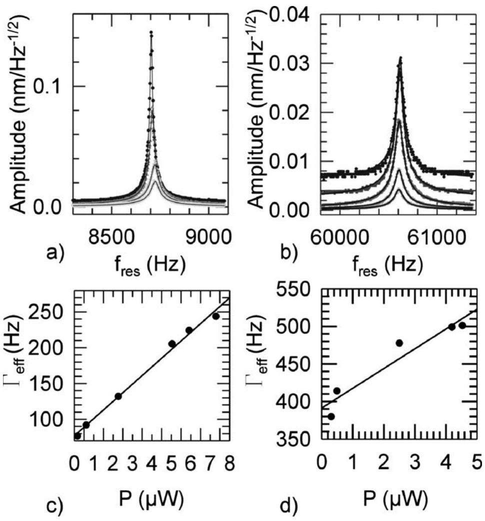

FIG. 7. (a) Cooling behavior of fundamental vibrational mode at 8.7 kHz. Laser powers coupled in the fiber before the cavity are 0.16 μW for Brownian peak, then 2.25, 5.8, and 7.6 μW, corresponding to 300, 174, 102, and 94 K, respectively. The fits were made according to Eq. (28). The effective damping for the spectra is shown in (c). (b) Cooling of the first harmonic at 60.6 kHz, with laser powers of 0.31, 0.49, 3.14, 4.19, and 4.53 μW corresponding to 300, 290, 251, 240, and 239 K, respectively. The offset of the spectra shows $1/\sqrt{P}$ dependence and is caused by the shot noise of the laser. (c) Effective damping Γ_{eff} with laser power before cavity for the ground mode at 8.7 kHz. Γ_{eff} shows linear power dependence according to Eq. (14). (d) Effective damping Γ_{eff} with laser power before cavity for the first harmonics at 60.6 kHz.

reflecting gold layer of 30 nm (yielding a reflectivity of 70%) to form the first cavity mirror. The divergent beam coming out of the fiber was collimated with a first lens with a numerical aperture of NA=0.25 (Geltech glass aspheric lens, diameter of 7.2 mm, focal length of 11.0 mm), then refocused on the sample with a second lens identical to the first one. The microscope yielded a Gaussian focus on the sample with a $1/e^2$ diameter of 6 μm. This diameter includes 86% of the Gaussian light mode. The sample is a cantilever with length of 223 μm, thickness of 470 nm, width of 22 μm, spring constant of $K=0.01$ N/m, and a gold layer of 42 nm, this time on one side only. A simulation of the silicon-gold bilayer system gave a reflectivity of 91%. The cavity finesse defined by the sample and the fiber end was $F=8$. Figure 7(a) shows cooling of the cantilever's first mode of vibration at 8.7 kHz from room temperature down to 94 K. The lowest effective temperature of 94 K was reached with the laser intensity of 7.6 μW (power coupled into fiber before first cavity mirror). This is by far not the maximal achievable power with the used laser. However, the cooling was limited by the appearance of instabilities in the static spring constant.[18]

A response measurement with weakly modulated laser done with the same procedure as described in Sec. V gave a value for the thermal diffusion time of $\tau=760$ μs and a ratio of $F_{\mathrm{pth}}/F_{\mathrm{rad}}\approx 4000$. An interesting point concerning photothermal cooling is shown in Fig. 7(b). The figure shows photothermally induced cooling of the cantilever's first harmonic, measured under the same conditions as the cooling of the ground mode shown in Fig. 7(a). This simultaneous cooling of two modes is very much consistent with the fact that the energy lost to the lowest vibration mode does not feed another mechanical mode of the cantilever but is transferred out of the system.

VII. PHOTOTHERMAL COOLING VERSUS RADIATION PRESSURE COOLING

In this section, we compare the lowest temperature reached with photothermal cooling and radiation pressure cooling. Both cooling methods are considered in optimal cooling condition at $\omega_0\tau=1$.

Photothermal cooling is always accompanied with optical absorption in the resonator limiting the system's temperature. Its advantages nevertheless are apparent because the light-induced force can be orders of magnitudes stronger than radiation pressure and the condition $\omega_0\tau=1$ can be reached by careful design of the gold layer on the cantilever or else by adjusting the bath temperature as shown in Sec. V. In experimental setups relying on radiation pressure cooling, the system still experiences residual absorption, heating up the resonator. Additionally, radiation pressure is by far not as strong as photothermal forces. To obtain a strong radiation pressure force, the light intensity in the cavity has to be increased considerably, leading in turn to increased absorption heat input to the resonator.

First, we address the situation of ideal cooling with radiation pressure without any residual absorption. As derived in Sec. III, the effective temperature is given by Eq. (32). In order to reach the minimum effective temperature, the cavity is tuned to the maximal gradient of radiation pressure,[18]

$$\nabla F_{\mathrm{rad,max}} \approx \frac{2P_0}{c\lambda}2\sqrt{R}g^2, \tag{41}$$

where P_0 is the laser power sent on the cavity. This maximal light-induced force gradient occurs at a detuning of $\lambda/(2\pi g\sqrt{3})$ from a cavity resonance.[18] With this expression and using the cavity storage time $\tau_{\mathrm{rad}}=L/[c(1-R)]$, the minimal effective temperature is found,

$$\frac{T_{\mathrm{eff,rad}}}{T} \approx \left(1 + \frac{1}{1+\omega_0^2\tau_{\mathrm{rad}}^2}\frac{P_0}{mc^2\Gamma}g^3\frac{L}{\lambda/2}\right)^{-1}. \tag{42}$$

Here, L is the cavity length. For a setup with $\omega_0\tau_{\mathrm{rad}}=1$, this simplifies to

$$\frac{T_{\mathrm{eff,rad}}}{T} = \left(\frac{P_0}{2mc^2\Gamma}\frac{L}{\lambda/2}g^3\right)^{-1} \tag{43}$$

for strong cooling $T_{\mathrm{eff}}\ll T$. No absorption of light in the mirror was taken into account up to now. The lowest temperatures can be achieved by increasing laser power and finesse, or else by choosing a system with low mass and damping as well as a large cavity length.

Now, we analyze cooling by photothermal forces. This effect is not only due to differential thermal expansion in a multilayered composite mirror surface, but can also originate from a nonuniform temperature distribution around the region where light is absorbed. In both cases the effect is not instantaneous and leads to time constants usually much larger than a single-pass time of flight of photons through the cavity. The effect can be seen as an effective force that displaces the mirror in proportion to the amount of the absorbed laser power. In order to compare photothermal forces with radiation pressure, we introduce an effective index n that accounts for a photothermally induced force F_{pth} that would scale like nF_{rad}, where $F_{\mathrm{rad}}=2P_0R/c$ is the force resulting from radiation pressure acting on the mirror. Since the photothermal force relies on the absorption α in the mirror, n is proportional to α. For illustration, the factor n for the doubly sided gold coated cantilever is -95, while for the cantilever coated on one side only it is 4000.

For better analogy with radiation pressure, where the delay time τ_{rad} scales as $L/[c(1-R)]$, we give the photothermal retardation time in units of τ_{rad} such that $\tau_{\mathrm{pth}}=n_\tau\tau_{\mathrm{rad}}$. Physically, n_τ represents the thermalization time constant of the mirror in units of τ_{rad}. For the first experiment shown in Sec. V, this parameter is 2.8×10^9; for the second experiment in Sec. VI, it is around 1.9×10^6.

With these definitions, the minimal effective temperature for photothermal cooling can be formulated with the help of Eq. (32) in the approximation of $\omega_0\tau=1$ and for strong cooling $T_{\mathrm{eff}}\ll T$,

$$\frac{T_{\mathrm{eff,pth}}}{T}=\left(nn_\tau\frac{P_0}{2mc^2\Gamma}\frac{L}{\lambda/2}g^3\right)^{-1}. \quad (44)$$

We stress that the effective indices n and n_τ are purely phenomenological. They are introduced here to allow a direct comparison between photothermal and radiation pressure cooling in terms of the ultimate cooling temperatures they yield.

We are now able to compare directly the minimal reachable temperatures and cooling power P_{cool} accounted for by radiation pressure and photothermal forces. In the dark and at thermal equilibrium, the lever's mechanical fluctuation dissipates its energy k_BT at a rate Γ. The dissipated power is therefore $(k_BT)\Gamma$ and is in equilibrium with the power that feeds the fluctuation as dictated by the fluctuation-dissipation theorem. When the mechanical resonator is cavity cooled, its vibrational effective temperature is T_{eff} but at the same time the internal source of mechanical dissipation Γ is still present. In other words, the internal mechanical dissipation rate that heats the resonator is still Γ. When the vibrational mode reaches a steady state at a temperature T_{eff}, the heat load in the mirror is $(k_BT_{\mathrm{eff}})\Gamma$. Consequently, in order to maintain a steady-state end temperature, the optical cooling extracts energy from the fluctuations in the mirror at a rate

$$P_{\mathrm{cool}}=k_B(T-T_{\mathrm{eff}})\Gamma. \quad (45)$$

Making use of Eq. (31), we obtain

$$P_{\mathrm{cool}}=k_BT\Gamma\left(1-\frac{\Gamma}{\Gamma_{\mathrm{eff}}}\right). \quad (46)$$

For large temperature differences that are typical for efficient cooling, we have $T_{\mathrm{eff}}\ll T$, which translates into $\Gamma_{\mathrm{eff}}\gg\Gamma$. The maximum cooling power is then approximated by $k_BT\Gamma$, which is interestingly still thermal mechanical fluctuation of a resonator in the dark. Until now, we did not consider any absorption in the mechanical resonator. Yet, real mirrors always have a finite absorption that acts as a heat source and leads to added fluctuation of the vibrational mode. As a result, it limits the lowest achievable temperature. The absorbed light heats the mirror body to reach a new temperature $T+\Delta T$, at which the excess temperature $\Delta T=\beta(\alpha P_{\mathrm{mirror}})$ is proportional to $\alpha P_{\mathrm{mirror}}$, the amount of absorbed laser power at the location of the mirror. Here, β is a proportionality factor that translates the absorbed power to an excess temperature and is dependent on the mirror's heat conduction and geometry properties. In a FP cavity, the laser power at the location of the mirror is larger than the laser power outside the cavity by an amount $P_{\mathrm{mirror}}=gP_0$ proportional to the cavity finesse. The excess temperature accounted for by residual absorption in the mirror corresponds to a heating power $P_{\mathrm{heat}}=k_B\Delta T\Gamma$ of the vibrational mode that ultimately balances the cooling power. The maximum laser power P_{max} usable before the absorption counteracts the cooling is obtained by equating $P_{\mathrm{cool}}=P_{\mathrm{heat}}$, which gives

$$P_{\mathrm{max}}=\frac{T}{\alpha\beta g}\left(1-\frac{\Gamma}{\Gamma_{\mathrm{eff}}}\right). \quad (47)$$

In the limit of strong radiation pressure cooling $\Gamma_{\mathrm{eff}}\gg\Gamma$ and cavities with $\omega_0\tau=1$, the relation for minimal temperature [Eq. (32)] for a cavity illuminated with the laser power P_{max} reads as

$$T_{\mathrm{min,rad}}=\left(\frac{P_0}{2mc^2\Gamma}\frac{L}{\lambda/2}\frac{g_{\mathrm{rad}}^2}{\alpha_{\mathrm{rad}}\beta_{\mathrm{rad}}}\right)^{-1} \quad (48)$$

for radiation pressure cooling and

$$T_{\mathrm{min,pth}}=\left(n_\tau n\frac{P_0}{2mc^2\Gamma}\frac{L}{\lambda/2}\frac{g_{\mathrm{pth}}^2}{\alpha_{\mathrm{pth}}\beta_{\mathrm{pth}}}\right)^{-1} \quad (49)$$

for photothermal cooling. The above derivation gives the means to compare radiation pressure cooling with photothermal cooling. One would intuitively think that the photothermal effect leads ultimately to heating and that only through radiation pressure cooling one could reach the lowest temperatures. This however needs to be substantiated with numbers as the parameters n, n_τ, α, and β can differ between both cooling methods by several decades. We offer here a direct comparison.

The surprising result is that photothermal cooling can have a higher cooling rate than radiation pressure cooling as long as $T_{\mathrm{pth}}<T_{\mathrm{rad}}$, which translates into the condition

$$\frac{\alpha_{\mathrm{pth}}\beta_{\mathrm{pth}}}{g_{\mathrm{pth}}^2n_\tau n}<\frac{\alpha_{\mathrm{rad}}\beta_{\mathrm{rad}}}{g_{\mathrm{rad}}^2}. \quad (50)$$

Because the absorption α scales as $1/g$, this can be reformulated as

$$\frac{\beta_{\mathrm{pth}}}{g_{\mathrm{pth}}^3n_\tau n}<\frac{\beta_{\mathrm{rad}}}{g_{\mathrm{rad}}^3}. \quad (51)$$

In the case of a single experiment with competing cooling mechanisms, we take $\beta_{\mathrm{pth}}=\beta_{\mathrm{rad}}$ and $g_{\mathrm{pth}}=g_{\mathrm{rad}}$. Then the condition for photothermal cooling to be superior over radiation pressure cooling is $n_\tau n > 1$. Typically, n lies in the range of several thousands, whereas n_τ can be designed to be as large as 10^{10}. To give an example for a mechanical resonator with $f_0 = 100$ MHz, a delay time of 1.6×10^{-9} s would be optimal. In a cavity with $g = 9$ ($R = 0.8$) and cavity length $L = 1$ mm, the photon storage time is only as low as 1.7×10^{-11} s. If the mirror is designed in a way that $n_\tau = 100$ and $n = 1000$, photothermal cooling is 10^5 times more efficient than radiation pressure cooling.

More generally, if one seeks the most promising mechanism to reach low temperatures, one would have to consider that n is proportional to the absorption $n = \xi\alpha$, with the constant ξ describing the distortion of the mirror with illumination. Then, one needs to compare

$$\frac{\beta_{\text{pth}}}{g_{\text{pth}}^2 n_\tau \xi} \quad \text{with} \quad \frac{\beta_{\text{rad}}}{g_{\text{rad}}^3}. \tag{52}$$

If we consider the case of $\beta_{\text{pth}} = \beta_{\text{rad}}$ for the sake of simplicity, one is left with a comparison of $g_{\text{pth}}^2 n_\tau \xi$ and g_{rad}^3. Should the realization of high value of n_τ and ξ, which rely solely on thermal and thermomechanical properties of the system, be easier to achieve than a corresponding improvement of the optical g, then photothermal effects would prove to be more efficient than radiation pressure to reach low temperatures and approach the oscillator's quantum ground state. For instance, in this work, with a low optical finesse cavity and with adequate thermal properties, we reached temperature reduction factors in the same range as that in Ref. 4 and as reported more recently in very high finesse cavities for radiation pressure.[8,9] Photothermal effects offer complementary perspectives to radiation pressure coupling in optomechanical experiments, be it for the technical improvement of optical cooling methods or for the design of new optomechanical devices.

VIII. CONCLUSION

We described a passive photothermal cooling mechanism. In our experiments with gold coated micromirrors, we were able to cool the thermal vibrations of the mirror from room temperature down to the range of 10 K. The back action mechanism involving a photothermal force time delayed with respect to any change in mirror position that enables this startling result was described in detail. A theoretical account on the delay time, in our case the time of heat conduction along the mirror, is given and shown to be in good agreement with instantaneous and delayed response measurements. We found that not only the lowest vibrational mode of the mirror is cooled by optical back action but higher modes as well. This result is consistent with the theory which indicates that the energy taken out of any vibrational mode is not transferred into other modes but irreversibly extracted out of the vibrating mirror. A comparison between cooling powers of experiments using radiation pressure and photothermal cooling is given. The conditions for which photothermal cooling leads to lower temperatures than those for radiation pressure cooling were specified in detail.

ACKNOWLEDGMENTS

We thank T. Hänsch, T. Kippenberg, and J. Kotthaus for fruitful discussions. This work was funded by Project No. NOMS KA 1216/2-1 of the Deutsche Forschungsgemeinschaft (DFG). I.F. acknowledges support of the Alexander von Humboldt Foundation.

---

*metzger@bu.edu
†ivan.favero@univ-paris-diderot.fr
‡karrai@lmu.de

[1] V. B. Braginsky and A. B. Manukin, *Measurement of Weak Forces in Physics Experiments* (University of Chicago, Chicago, 1977).
[2] V. B. Braginsky, S. E. Strigin, and S. P. Vyatchanin, Phys. Lett. A **287**, 331 (2001).
[3] V. B. Braginsky and S. P. Vyatchanin, Phys. Lett. A **279**, 154 (2001).
[4] C. Metzger and K. Karrai, Nature (London) **432**, 1002 (2004).
[5] A. Dorsel, J. D. McCullen, P. Meystre, E. Vignes, and H. Walther, Phys. Rev. Lett. **51**, 1550 (1983).
[6] W. Marshall, C. Simon, R. Penrose, and D. Bouwmeester, Phys. Rev. Lett. **91**, 130401 (2003).
[7] S. Gigan, H. R. Böhm, M. Paternostro, F. Blaser, G. Langer, J. B. Hertzberg, K. C. Schwab, D. Bäuerle, M. Aspelmeyer, and A. Zeilinger, Nature (London) **444**, 67 (2006).
[8] O. Arcizet, P. F. Cohadon, T. Briant, M. Pinard, and A. Heidmann, Nature (London) **444**, 71 (2006).
[9] A. Schliesser, P. Del'Haye, N. Nooshi, K. J. Vahala, and T. J. Kippenberg, Phys. Rev. Lett. **97**, 243905 (2006).
[10] I. Favero, C. Metzger, S. Camerer, D. König, H. Lorenz, J. P. Kotthaus, and K. Karrai, Appl. Phys. Lett. **90**, 104101 (2007).
[11] P. F. Cohadon, A. Heidmann, and M. Pinard, Phys. Rev. Lett. **83**, 3174 (1999).
[12] J. Mertz, O. Marti, and J. Mlynek, Appl. Phys. Lett. **62**, 2344 (1993).
[13] S. Mancini, D. Vitali, and P. Tombesi, Phys. Rev. Lett. **80**, 688 (1998).
[14] D. Vitali, S. Mancini, L. Ribichini, and P. Tombesi, Phys. Rev. A **65**, 063803 (2002).
[15] D. Kleckner and D. Bouwmeester, Nature (London) **444**, 75 (2006).
[16] F. Marquardt, J. G. E. Harris, and S. M. Girvin, Phys. Rev. Lett. **96**, 103901 (2006).
[17] M. Poggio, C. L. Degen, H. J. Mamin, and D. Rugar, Phys. Rev. Lett. **99**, 017201 (2007).
[18] M. Vogel, C. Mooser, R. J. Warburton, and K. Karrai, Appl. Phys. Lett. **83**, 1337 (2003).
[19] B. C. Barish and R. Weiss, Phys. Today **52**(10), 44 (1999).
[20] A. Naik, O. Buu, A. D. Armour, A. A. Clerk, M. P. Blencowe, and K. C. Schwab, Nature (London) **443**, 193 (2006).
[21] R. Fitzgerald, Phys. Today **59**(11), 19 (2006).

[22] T. Corbitt, C. Wipf, T. Bodiya, D. Ottaway, D. Sigg, N. Smith, S. Whitcomb, and N. Mavalvala, Phys. Rev. Lett. **99**, 160801 (2007).
[23] J. D. Thompson, B. M. Zwickl, A. M. Jayich, F. Marquardt, S. M. Girvin, and J. G. E. Harris, Nature (London) **452**, 72 (2008).
[24] T. W. Hänsch and A. Schawlow, Opt. Commun. **13**, 68 (1975).
[25] C. Cohen-Tannoudji and W. Phillips, Phys. Today **43**(10), 33 (1990).
[26] V. B. Braginsky, S. E. Strygin, and S. P. Vyatchanin, Phys. Lett. A **287**, 331 (2001).
[27] R. E. Mihailovich and N. C. MacDonald, Sens. Actuators, A **50**, 199 (1995).
[28] R. Sandberg, K. Molhave, A. Boisen, and W. Svendsen, J. Micromech. Microeng. **15**, 2249 (2005).
[29] J. R. Barnes, R. S. Stephenson, C. N. Woodburn, S. J. O'Shea, M. E. Welland, T. Rayment, J. K. Gimzewski, and C. Gerber, Rev. Sci. Instrum. **65**, 3793 (1994).
[30] J. K. Gimzewski, C. Gerber, E. Meyer, and R. R. Schlittler, Chem. Phys. Lett. **217**, 589 (1994).
[31] R. Sandberg, W. Svendsen, K. Molhave, and A. Boisen, J. Micromech. Microeng. **15**, 1454 (2005).
[32] INSPEC, The Institution of Electrical Engineers, 1988.